

# The 21 cm Signature of Shock Heated and Diffuse Cosmic String Wakes

Oscar F. Hernández<sup>1,2</sup> and Robert H. Brandenberger<sup>2</sup>

1) Marianopolis College, 4873 Westmount Ave., Westmount, QC H3Y 1X9, Canada

2) Department of Physics, McGill University, Montréal, QC, H3A 2T8, Canada

The analysis of the 21 cm signature of cosmic string wakes is extended in several ways. First we consider the constraints on  $G\mu$  from the absorption signal of shock heated wakes laid down much later than matter radiation equality. Secondly we analyze the signal of diffuse wake, that is those wakes in which there is a baryon overdensity but which have not shock heated. Finally we compare the size of these signals to the expected thermal noise per pixel which dominates over the background cosmic gas brightness temperature and find that the cosmic string signal will exceed the thermal noise of an individual pixel in the Square Kilometre Array for string tensions  $G\mu > 2.5 \times 10^{-8}$ .

PACS numbers: 98.80.Cq

## I. INTRODUCTION

In a previous paper [1] we studied the signal of a shock heated cosmic string wake in a position space 21cm redshift maps. We pointed out that cosmic string wakes give rise to a pronounced signal in such maps, in particular at redshifts larger than that of conventional reionization. The signal of a single wake is a wedge which is extended (a degree or larger for redshifts of  $z \sim 20$ ) in both angular directions and thin in redshift direction. This effect comes from the fact that wakes form overdensities in baryons already at very high redshifts, and that these regions then lead to the extra 21cm emission or absorption.

In a followup paper [2] we computed the angular power spectrum for shock heated cosmic string wakes emitting 21 cm radiation. Because of our interest in shock heating in both [1] and [2] we focused our attention on those wakes with the greatest kinetic gas temperature  $T_K$ . Thus we concentrated our analyses on the wakes formed earliest,  $z_i \sim 3000$  and emitting 21 cm radiation as late as possible before reionization,  $z_e \sim 20$ . This led us to miss the constraints on  $G\mu$  that shock heated wakes formed at later  $z_i$  could provide by considering the absorption of 21 cm radiation. In this paper we consider these constraints.

Furthermore, even if baryons collapsing onto the primordial string wake do not shock heat, the string will nevertheless induce an overdense region of baryons. This region, however, will be more diffuse than if shock heating occurs. The wakes will be thicker but the overdensity smaller. In this paper, we study the 21cm signal of such a “diffuse” cosmic string wake.

Current constraints on the cosmic string tension from analyses of the angular power spectrum of CMB anisotropy maps yield

$$G\mu < 1.5 \times 10^{-7} \tag{1}$$

using combined data from WMAP and SPT microwave experiments [3]. Limits based only on WMAP data gives a bound larger than this by a factor of two [4]. It must be emphasized that any limits on  $G\mu$  coming from power spectra analyses implicitly depend on parameters describing the cosmic string scaling solution which are quite uncertain. Two prime examples of such parameters are the number  $N$  of string segments crossing any Hubble volume, and the curvature radius  $c_1$  of a long string relative to the Hubble radius. These parameters are known only to within an order of magnitude since they must be determined via numerical simulations of cosmic string network evolution, and these simulations are extremely challenging because of the huge hierarchy of scales which must be included at the same time.

In our analyses below we show that a cosmic string signal will exceed the thermal noise of an individual pixel in a future radio telescope such as the Square Kilometre Array (SKA) for a string tension

$$G\mu > 2.5 \times 10^{-8} . \tag{2}$$

Our new limit is independent of the parameters  $N$  and  $c_1$ . In addition, since the signal of a string wake has a very special geometry in position space, position space shape detection algorithms are likely to be able to detect string wake signals even if they do not stick out above the Gaussian noise on a pixel by pixel basis. The situation is similar to what is encountered when searching for cosmic string signals in CMB anisotropy maps: since long string segments produce line discontinuities in the maps, these can be identified by edge detection algorithms such as the Canny algorithm [5] for values of the tension substantially lower than the value for which the string signal dominates on a pixel by pixel basis, as has been studied in detail in [6].

The paper is organized as follows: We begin in Section II with a brief review of cosmic strings, their wakes, and their 21 cm signatures. Readers familiar with such results may skip this section. Section III is the main part of our work. In this section we extend the analysis of the 21 cm signature of cosmic string wakes in several ways. First we consider the constraints on  $G\mu$  from the absorptions signal of shock heated wakes laid down much later than matter radiation equality. Secondly we analyze the signal of diffuse wakes, that is those wakes in which there is a baryon overdensity but which have not shock heated. Finally we compare the size of these signals to the expected thermal noise per pixel which dominates over the background cosmic gas brightness temperature. In Section IV we present our conclusions and put our work in context.

## II. COSMIC STRINGS, THEIR WAKES AND 21 CM SIGNATURES

Many particle physics models beyond the Standard Model predict the existence of cosmic strings. In particular, cosmic strings are produced at the end of inflation in many models of brane inflation [7] and in many supergravity models [8]. Cosmic strings may also survive in early universe models based on superstring theory such as “string gas cosmology” [9, 10]. Since the amplitude of cosmological signatures of cosmic strings is proportional to the string tension, which itself is set by the energy scale of the new physics, searching for signatures of strings in cosmology is a way of probing Beyond the Standard Model physics which is complementary to accelerator probes such as the Large Hadron Collider experiments which probe the low energy limit of such theories.

Cosmic strings can be used as a cosmological probe of New Physics because any particle physics model which admits stable cosmic strings as a solution inevitably results in a network of such strings forming during a symmetry breaking phase transition in the early universe (see [11–13] for reviews on cosmic strings and cosmology). Such a network will persist to the present time and approaches a dynamical attractor configuration, the so-called “scaling solution” in which the statistical properties of the string network are independent of time if all lengths are scaled to the Hubble radius. The cosmic string scaling solution is characterized by a random-walk-like network of infinite (or “long”) strings with step length comparable to the Hubble radius, plus a distribution of cosmic string loops with radii smaller than the Hubble radius. The typical transverse velocity of a long string segment is the speed of light. This implies that at all times  $t > t_{eq}$  ( $t_{eq}$  being the time of equal matter and radiation) relevant for structure formation there are strings which act as seeds for the accretion of matter. The key parameter which characterizes cosmic strings and their cosmological consequences is the mass per unit length  $\mu$ . It is usually quoted in terms of the dimensionless number  $G\mu$ , where  $G$  is Newton’s gravitational constant.

Both long string segments and string loops lead to nonlinearities in the matter distribution at all redshifts up to  $z_{eq}$ , the redshift of equal matter and radiation. Cosmic string network simulations [14] indicate that the long strings have a larger effect than the loops, so we will here focus our attention on the effects of long string segments, as we did in [1, 2] (For a recent study of the 21cm signal of a cosmic string loop see [15]). In the standard  $\Lambda$ CDM cosmology without strings, nonlinear structures are negligible until shortly before the time of reionization. Hence, the signals of cosmic strings should be more and more pronounced against the “noise” of effects from structure formation in the  $\Lambda$ CDM model the higher the redshift is. 21cm surveys hence appear as an ideal window to probe for the possible existence of cosmic strings. They probe the distribution of matter at much higher redshifts than galaxy redshift surveys since they map out the distribution of neutral hydrogen in the universe, in particular before the time of reionization. Compared to CMB maps, 21cm maps have the advantage of yielding three-dimensional information.

The nonlinearity in the matter distribution induced by a long string segment at time  $t$  takes the form of a “wake” [16] whose length is set by the length of the string segment (which will be similar to the Hubble radius  $t$ ), whose width is set by  $v_s \gamma_s t$ , where  $v_s$  is the transverse velocity of the string segment and  $\gamma_s$  is the associated relativistic gamma factor, and whose average thickness is proportional to  $G\mu t$ . The wake formation starts with an initial velocity perturbation and then grows by gravitational accretion.

The velocity perturbation (see Figure 1) stems from the fact that space perpendicular to a long string segment is conical, i.e. flat space with a missing wedge whose deficit angle is  $\alpha = 8\pi G\mu$ . A string moving through a gas of particles with transverse velocity  $v_s$  will hence induce a velocity perturbation  $\delta v$  of the gas towards the plane behind the string, whose magnitude is given by  $\delta v = 4\pi G\mu v_s \gamma_s$ .

A cosmic string segment laid down at time  $t_i$  (we are interested in  $t_i \geq t_{eq}$ ) will generate a wake with physical dimensions:

$$l_1(t_i) \times l_2(t_i) \times w(t_i) = t_i c_1 \times t_i v_s \gamma_s \times t_i 4\pi G\mu v_s \gamma_s. \quad (3)$$

where  $c_1$  is a constant of order one. In the above, the first dimension is the length in direction of the string, the second is the depth, and the third is the average width. After being laid down, the wake will grow by gravitational accretion. This has been studied using the Zel’dovich approximation [17] in a number of works [18]. In this method of analysis, we follow the time evolution of the height above the centre of the wake of mass shells to determine the

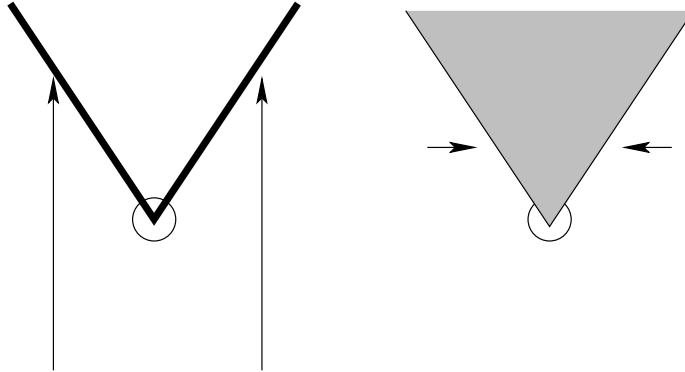


FIG. 1: Sketch of the mechanism by which a wake behind a moving string is generated. Consider a string perpendicular to the plane of the graph moving straight downward. From the point of view of the frame in which the string is at rest, matter is moving upwards, as indicated with the arrows in the left panel. From the point of view of an observer sitting behind the string (relative to the string motion) matter flowing past the string receives a velocity kick towards the plane determined by the direction of the string and the velocity vector (right panel). This velocity kick towards the plane leads to a wedge-shaped region behind the string with twice the background density (the shaded region in the right panel).

comoving distance  $q_{nl}$  which “turns around” at time  $t$ , i.e. for which the physical height  $h(q, t)$  is maximal. We obtain that the comoving thickness grows linearly with the scale factor of the universe. A wake laid down at redshift  $z_i$  will have comoving thickness at redshift  $z$  given by

$$q_{nl}(z) = \frac{16\pi}{5} \frac{G\mu v_s \gamma_s}{H_o} (z_i + 1)^{1/2} \frac{1}{(z + 1)}. \quad (4)$$

The physical height of the shell above the centre of the wake at the time of “turnaround” is half what the height would be in the absence of gravitational accretion, and hence the relative overdensity is a factor of 2. It is then assumed that the shell collapses to half of the height it had at turnaround, that it then undergoes shocks and virializes at that distance. Then, the overdensity will be a factor of 4 greater than the background density. This approximate analytical analysis has been confirmed in detailed hydrodynamical simulations [19].

During the infall onto the string wake, the baryons acquire kinetic energy which during the process of shock heating transforms to thermal energy. The kinetic temperature  $T_K$  acquired by the hydrogen atoms can be obtained from the kinetic energy which particles acquire when they hit the shock front. This is determined using the Zel’dovich approximation [17]. The result obtained in [1] is

$$T_K \simeq [20 \text{ K}] (G\mu)_6^2 (v_s \gamma_s)^2 \frac{z_i + 1}{z + 1}, \quad (5)$$

where  $(G\mu)_6$  indicates the value of  $G\mu$  in units of  $10^{-6}$ . The result is expressed in degrees Kelvin.

Note that the wake kinetic temperature increases as  $z$  decreases since the wakes have more time to grow, which in turn leads to a growing gravitational potential. Since  $T_\gamma$  decreases in time, then it is more and more likely that the string wake 21cm signal will be in emission rather than absorption as  $t$  increases. However, it turns out that for redshifts significantly larger than that of conventional reionization and for string tensions smaller than the current limit (1),  $T_K$  is smaller than  $T_\gamma$  and that hence the string wake signal will be in absorption.

The 21cm signal of a cosmic string wake has a distinctive geometry. We will see the string-induced absorption (or emission) regions in directions of the sky where our past light cone intersects the cosmic string wake. These are wedges in the sky of angular scale determined by the comoving Hubble radius at the time that the string is formed. The string wake grows in thickness, but its planar dimensions are constant in comoving coordinates. For wakes formed at a redshift corresponding to recombination this angular scale is about one degree, for wakes formed at equal matter and radiation slightly smaller. Since photons emitted at the top and bottom of the wake undergo slightly different redshifts, the region in 21cm redshift surveys of extra emission/absorption takes on the form of a thin wedge in redshift direction with a thickness which is [1]

$$\left| \frac{\delta z}{z + 1} \right| = \left| \frac{\delta \nu}{\nu} \right| = \frac{24\pi}{15} G\mu v_s \gamma_s \frac{(z_i + 1)^{1/2}}{(z + 1)^{1/2}}, \quad (6)$$

### III. DIFFUSE COSMIC STRING WAKES

The analysis in the previous section neglected the temperature of the gas at the time that the wake was formed. The accretion onto a string wake further increases the intrinsic gas velocities, leading to an effective gas temperature which is  $2.5T_g$ , where  $T_g$  is the temperature of the background gas. If

$$T_K < 2.5 \times T_g, \quad (7)$$

then the incoherent velocities due to the thermal motion of the accreted gas dominate over the coherent velocity induced by accretion. In this case, there is no shock heating, and the thickness of the overdense region induced by the wake is larger than it would be in the absence of thermal motion of the gas particles. The resulting overdense region we will call a “diffuse wake”.

We now estimate the size of the diffuse wake. In linear cosmological perturbation theory, the total mass accreted by the string wake is the same both in the cases with and without shock heating. The difference is that the large intrinsic thermal gas velocity will render the wake wider and hence less dense.

The first step is to compute the width  $h_w$  of the wake obtained taking into account the gas temperature  $T_g$ . The result is

$$h_w(z)|_{T_K < T_g} = h_w(z)|_{T_g=0} \left( \frac{T_g}{T_K} \right) \quad (8)$$

for  $T_K < T_g$ . The diffuse wake will thus be thicker by the ratio of temperatures  $T_g/T_K$ , but the density of baryons will be smaller by the same factor. Hence, the width of the 21cm signal induced by a diffuse wake will be thicker in redshift direction by the above ratio of temperatures compared to what is given in (6). On the other hand, the 21cm brightness temperature will be smaller since it is proportional to the baryon density which is smaller than in the case of a shock-heated wake.

The formula (8) for the width of a diffuse wake can be derived by assuming equipartition of energy between thermal energy and potential energy which for  $T_K \ll T_g$  yields

$$m_{HI} \delta\Phi = \frac{3}{2} T_g, \quad (9)$$

where  $m_{HI}$  is the mass of a hydrogen atom and  $\delta\Phi$  is the gravitational potential induced by the wake. The latter, in turn, is

$$\delta\Phi = 2\pi G\sigma|h|, \quad (10)$$

where  $\sigma$  is the surface density of the wake, and  $|h|$  is the height. Combining (9) with (10) yields the linear scaling in temperature given in (8).

The surface density  $\sigma$  of a diffuse wake is the same as that of a shock heated wake. It is given by the energy per unit area of matter within a comoving height  $q_{nl}(z)$ , the shell which is turning around at redshift  $z$ . Thus  $\sigma(z) = q_{nl}(z)\rho_0$ , where  $\rho_0$  is the current background density. The overdensity  $\Delta\rho$  in the diffuse wake is given by

$$\Delta\rho(z) = \frac{\sigma(z)}{h_w(z)} = \rho_0 \left( \frac{T_K}{T_g} \right). \quad (11)$$

which results in

$$\frac{\rho}{\rho_0} = \left( 1 + \frac{T_K}{T_g} \right). \quad (12)$$

The extra baryon density in the wake leads to extra 21 cm absorption or emission.

The expression for the wake brightness temperature written in terms of kinetic temperature  $T_{Kg}$  and the hydrogen atom number density  $n_{HI}$  is very similar for a shock heated or a diffuse wake. The only difference is that  $T_{Kg}$  is the kinetic temperature  $T_K$  of the wake when shock heating occurs whereas it should be interpreted as the kinetic temperature of the cosmic gas  $T_g$  for diffuse wakes.

$$\delta T_b(z_e) = [17 \text{ mK}] \frac{x_c}{1+x_c} \left( 1 - \frac{T_\gamma}{T_{Kg}} \right) \frac{n_{HI}^{wake} (1+z_e)^{1/2}}{n_{HI}^{bg} 2 \sin^2 \theta}. \quad (13)$$

Here,  $z_e$  is the redshift of 21 cm emission or absorption,  $T_\gamma$  is the CMB temperature,  $\theta$  is the angle of the 21 cm ray with respect to the vertical to the wake, and  $x_c$  are the collision coefficients whose values can be obtained from

the tables listed in [20]. Here and throughout we take the cosmological parameters to be  $H_0 = 73 \text{ km s}^{-1} \text{ Mpc}^{-1}$ ,  $\Omega_b = 0.0425$ ,  $\Omega_m = 0.26$ . We work with a matter dominated universe for  $z \leq 3000$  with the age of the universe  $t_0 = 4.3 \times 10^{17} \text{ s}$ . The origin of the  $\sin^{-2}(\theta)$  factor will be discussed in the Appendix, where it will also be shown that this factor does not lead to any physical divergence.

For a shock heated wake, the ratio of the wake's hydrogen atom number density to the background density,  $n_{HI}/n_{HI}^{bg}$ , is 4. For a diffuse wake the relative brightness temperature is lower than for a wake which has undergone shock heating since the number density  $n_{HI}$  of hydrogen atoms inside the diffuse wake is smaller, and thus its ratio in (13) to the background density  $n_{HI}^{bg}$  is smaller. For our analysis below we take:

$$\frac{n_{HI}}{n_{HI}^{bg}} = \left(1 + \frac{T_K}{T_g}\right) \quad T_K \leq 3T_g \quad (14)$$

$$= 4 \quad T_K \geq 3T_g \quad (15)$$

Note that for simplicity we have used  $T_K \leq 3T_g$  instead of  $T_K \leq 2.5T_g$ .

The brightness temperature signal in (13) discussed in [1, 2] was compared to the average brightness temperature of the surrounding cosmic gas. Between redshift  $z = 20$  and 35 the average background brightness temperature varies from -0.34 mK to -8.6 mK, respectively. However the analysis of the signal did not consider beam size nor thermal noise. In fact for  $z \sim 20$  it is the thermal noise, and not the background brightness temperature, that will first limit our ability to detect a cosmic string wake signal. The opposite is true for  $z = 35$ . Beam size and thermal noise for the 21 cm brightness temperature were considered in [21] where their Eq. (4.19) gives the thermal noise per pixel:

$$T_n = \frac{12 \text{ mK (arcmin}/\theta_{\text{resolution}})}{\sqrt{(\tau/10^4\text{hr})(A_e/\text{km}^2)}} \left(\frac{1+z}{21}\right)^{3.85} \left[\frac{\sqrt{1+z}}{\sqrt{1+z-1}}\right]^{1/2} \quad (16)$$

Here  $\tau$  is the total observing time and  $A_e$  is the effective antenna area. To derive this noise temperature per pixel in [21] we began with the thermal noise per visibility as given by Morales [22] to arrive at the thermal noise per pixel for the brightness temperature. The angular resolution is  $\lambda/D$  where  $\lambda$  is the observation frequency and  $D$  is the baseline. The angular resolution is assumed to be tuned by a dilution of the array from being fully compact by a simple scaling of all baseline positions by a fixed amount. The system temperature is given by ARCADE 2 [23]. Further details can be found in [21].

The noise per pixel resolution dependence given in eq. 16 assumes an isotropic resolution in all three spatial directions. However for a cosmic wake signal, the width is order  $4\pi G\mu(z_i+1)/(z+1)$  smaller than the two length directions, whereas each length direction is of order the Hubble size. If  $\theta_{\text{hubble}}(z)$  is the angular resolution needed for the wake's length, then  $\theta_{\text{hubble}}(z)4\pi G\mu(z_i+1)/(z+1)$  is the angular resolution needed for the width. Thus an appropriate estimate of the resolution in radians needed to calculate the noise per pixel is:

$$\theta_{\text{resolution}}(z) = \left(\frac{4\pi G\mu(z_i+1)}{(z+1)}\right)^{1/3} \theta_{\text{hubble}}(z) = \left(\frac{4\pi G\mu(z_i+1)}{(z+1)}\right)^{1/3} \frac{1}{(\sqrt{z+1}-1)} \quad (17)$$

Hence, in a three dimensional map with the necessary resolution to detect a cosmic string wake laid down at  $z_i$  and emitting or absorbing radiation at  $z$ , the thermal noise per pixel is:

$$T_n^{\text{wake}} = \frac{0.19 \text{ mK } (G\mu)_9^{-1/3} (z_i+1)^{-1/3}}{\sqrt{(\tau/10^4\text{hr})(A_e/\text{km}^2)}} \left(\frac{z+1}{21}\right)^{4.68} (1-1/\sqrt{z+1})^{1/2} \quad (18)$$

where  $(G\mu)_9 \equiv 10^9 G\mu$ .

We will consider 10 000 hours of total observing time. Evidently for the SKA the effective antenna area is 1 sq km. For  $z_i = 3000$  and  $z = 20$ , a  $G\mu = 4 \times 10^{-8}$  leads to an average noise per pixel  $T_n = 0.3 \text{ mK}$  comparable in size to the background brightness temperature. Smaller  $G\mu$  require a smaller resolution and lead to larger noise per pixel. Hence for  $G\mu < 4 \times 10^{-8}$  the thermal noise dominates over the background brightness temperature for the wake signal. For example at  $z_i = 3000$  and  $z = 20$  a  $G\mu = 5 \times 10^{-9}$  gives a  $\theta_{\text{resolution}}(z) = 5.8 \times 10^{-3}$  radians, which is 20 minutes of arc, and hence an average noise per pixel of  $T_n = 0.66 \text{ mK}$ . For strings laid down at a lower redshift the noise is greater. The noise is also a rising function of the emission redshift  $z$ . For a  $z_i = 1000$  with  $z = 20, 25$  and 35,  $T_n = 1.6 \text{ mK}, 2.0 \text{ mK}$  and  $2.7 \text{ mK}$ , respectively.

In Figure 2 we show the relative brightness temperature (vertical axis) as a function of  $(G\mu)_6$  (horizontal axis) for various values of the redshift  $z_i$  of wake formation, evaluated at the redshift  $z = 20$ . Negative (positive) brightness temperature means absorption (emission). The two almost horizontal (brown) lines give the noise per pixel level in an experiment such as the SKA for the pixel size chosen such as to optimize the search for a string wake with the respective value of  $G\mu$  (see the above discussion).

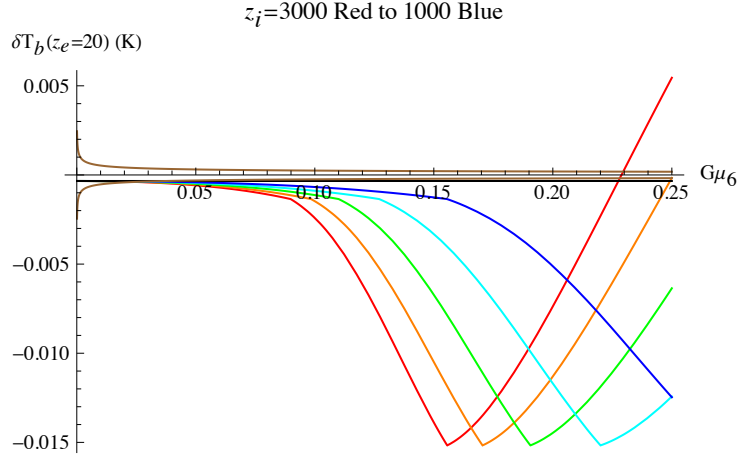


FIG. 2: The relative brightness temperature (vertical axis) in degrees Kelvin as a function of  $(G\mu)_6$  (horizontal axis) for various values of the formation redshift  $z_i$ , evaluated for an observation redshift of  $z = 20$ . The curves from left to right (in the region of low values of  $G\mu$ ) correspond to  $z_i = 3000$  (red curve),  $z_i = 2500$  (orange),  $z_i = 2000$  (green),  $z_i = 1500$  (light blue) and  $z_i = 1000$  (dark blue). The two brown lines indicate the expected thermal noise per pixel in an experiment such as the SKA, with a pixel size chosen to depend on  $G\mu$  as described in the text. The black line that is almost indistinguishable from the x-axis is the brightness temperature of the background cosmic gas.

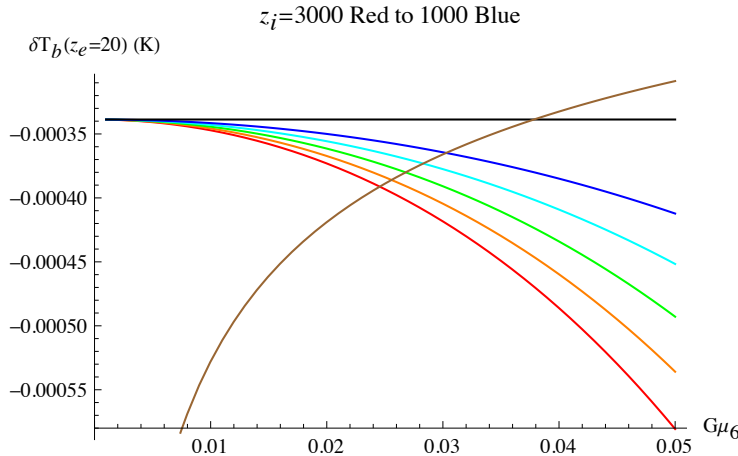


FIG. 3: A zoom in of figure 2 to the point where the noise curve (brown) crosses the signal curves (colours red to blue). The black line at the top of the graph is the brightness temperature of the background cosmic gas.

As expected, the larger the value of  $z_i$ , the easier it is to detect low values of  $G\mu$  since the wakes have had a longer time to grow in thickness. A feature overlooked in our previous work [1, 2] is that for a fixed observational redshift  $z$ , there will be a range of values of  $G\mu$  for which the wake's brightness temperature  $T_K$  will be so close to the background cosmic gas temperature that there will be no signal. In this situation, we can consider smaller values of  $z_i$  which lead to a clean and large absorption signal.

For each curve in Figure 2 it is apparent that there is a kink in the brightness curve (in the absorption region). This kink occurs at the value of  $G\mu$  for which  $T_K = 3T_g$ , the transition point between a wake with shock heating (larger values of  $G\mu$ ) and a diffuse wake. Our previous analysis was only valid until that point. We see here that with our current work it is possible to extend the range of values of  $G\mu$  which can be probed by 21cm redshift surveys.

Taking into account that the optimal pixel size will depend on  $G\mu$ , then the pixel noise level will also depend on  $G\mu$ . In Figure 3 we zoom in on the small  $G\mu$  region of the previous figure and compare the string signal to the pixel noise. We see that the absorption signal of the diffuse wakes is larger than the noise level for values of  $G\mu$  larger than

$$G\mu > 2.5 \times 10^{-8} \quad (19)$$

for a detection redshift of  $z = 20$ . This is an improvement of the current bound (1) and demonstrates the potential of 21cm surveys to probe cosmic strings.

For smaller values of  $G\mu$ , cosmic string wakes will still provide a signal. The signal has a particular shape in a three-dimensional redshift survey and should hence be detectable using shape detection algorithms for values of  $G\mu$  much smaller than the above value (19). In work in progress we are exploring this issue quantitatively. Note that a similar problem arises in the case of identifying cosmic string signatures in CMB temperature maps. It was shown [6] that edge detection algorithms provide the promise of pushing the limits of detection several orders of magnitude below the level of the pixel noise, and one order of magnitude lower than limits which can be achieved using CMB angular power spectra studies. Thus, we are optimistic that 21cm redshift surveys will provide a very promising arena to probe for the possible existence of cosmic strings.

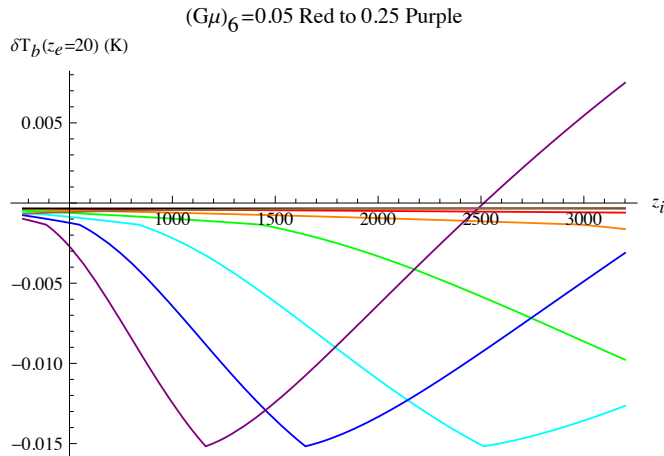


FIG. 4: The relative brightness temperature (vertical axis) as a function of formation redshift  $z_i$  (horizontal axis) for various values of  $(G\mu)_6$ . The values of  $(G\mu)_6$  chosen are 0.05, 0.09, 0.13, 0.17, 0.21, and 0.25 (red, orange, green, light blue, dark blue and purple curves, respectively). At low values of  $z_i$  some of these curves are labelled by an increasing amplitude of the absorption signal. The black and brown lines near the x-axis represents the background gas brightness temperature and the noise temperature, respectively. They are nearly indistinguishable on this scale for these values of  $G\mu$ . The noise is plotted for  $(G\mu)_6 = 0.05$ . The larger values of  $(G\mu)_6$  would give less noise.

In Figure 4 we show how that formation redshift which leads to the largest amplitude of the absorption signal depends on  $z_i$ . If we are looking for strings of a particular value of  $G\mu$  we would be focusing on wakes formed at the redshift which yields largest absorption amplitude. Since the formation redshift determines the size of the 21cm wedge which the corresponding wake produces, we can use the size information to optimize the search strategy.

#### IV. CONCLUSIONS

We have extended the analysis of the 21cm signal of cosmic string wakes to the case when the string tension is too small to yield shock heating of the wake. Instead, a “diffuse wake” forms. This wake is less dense but thicker than a wake which has undergone shock heating. Hence, the relative 21cm brightness temperature is smaller in amplitude, but it is extended over a larger redshift interval.

Demanding that the relative brightness temperature exceeds the pixel thermal noise in a future 21cm experiment such as the Square Kilometre Array (SKA) (with the pixel size chosen to be able to identify the wake signal, as described in the text) leads to a limit of  $G\mu > 2.5 \times 10^{-8}$ , an improvement over the current limit of Eq. (1) obtained from CMB anisotropy maps [3]. There are three important comments to make. First, a limit obtained by direct searches in position space is independent of some of the unknown parameters characterizing the scaling solution of strings (for example, it is largely independent of the number of strings per Hubble volume), whereas a bound obtained from the angular correlation function of CMB anisotropies depends on these parameters. Thus, a bound obtained by the methods we describe is more robust. Secondly with more statistics, even a signal strength below the noise can be detected. And finally, since cosmic string wakes produce signals with a distinguished geometry (namely thin wedges in redshift maps), these signals should be detectable by clever statistical techniques even if the amplitude is substantially smaller than the pixel noise. An example of a statistical tool which could be used to look for the specific string wake signal is the set of Minkowski functionals, statistics designed to characterize the topology of the structure of maps. For a preliminary study of this approach with references to the original literature see [24].

## V. APPENDIX

In this appendix we present how the  $(\sin \theta)^{-2}$  factor in the expression for the wake brightness temperature arises from the line profile term  $\phi(\nu)$ . We also explain why it does not imply any physical singularity in the limit  $\theta \rightarrow 0$ .

We begin with the formula for the relative brightness temperature of photons (see [1] and references therein)

$$\delta T_b(\nu) \simeq \frac{(T_S - T_\gamma)}{(1+z)} \tau_\nu, \quad (20)$$

where the optical depth  $\tau_\nu$  is given by

$$\tau_\nu = \frac{3c^2 A_{10}}{4\nu^2} \left( \frac{\hbar\nu_{10}}{k_B T_S} \right) \frac{N_{HI}}{4} \phi(\nu). \quad (21)$$

Here  $N_{HI}$  is the column density of HI, and  $\phi(\nu)$  is the line profile.

The line profile accounts for the nonzero width of the 21 cm line. The line profile is a sharply peaked function about  $\nu_{21} = 1420$  MHz normalized such that

$$\int_0^\infty \phi(\nu) d\nu = 1 \quad (22)$$

For the case at hand the line profile is not a Dirac delta function because the Hubble expansion leads to a velocity gradient along the line of sight. Due to this radial velocity gradient, the emitted 21 cm photons incur a local line broadening which one can interpret as a relative Doppler shift.

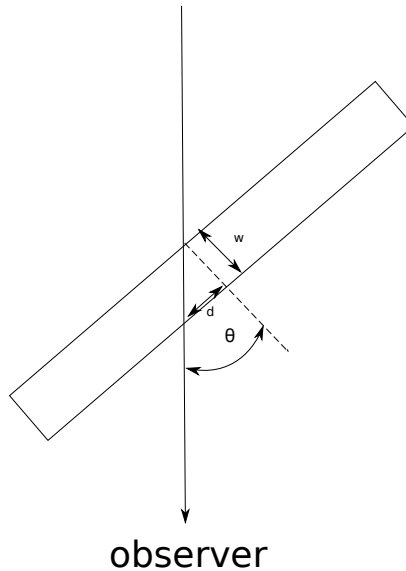


FIG. 5: A 21 cm light ray traverses a cosmic string wake of width  $w$ .

In particular, let us consider photons reaching us at an angle  $\theta$  relative to the vertical of the wake having width  $w$  (see fig. 5). There is a relative Doppler shift  $\delta\nu$  between photons from the front and back of the wake along the photon trajectory. The horizontal distance  $d$  along the wake between the back point of the photon trajectory and the photon trajectory exiting the wake is given by

$$d = w \tan \theta. \quad (23)$$

The relative Doppler shift is due to the Hubble expansion of the planar dimensions of the wake. Thus, the component of this expansion velocity in direction of the photon trajectory is given by

$$v_{//} = Hd \sin \theta = \frac{Hw \sin^2 \theta}{\cos \theta}, \quad (24)$$



and we have a frequency width given by

$$\delta\nu = v_{//} \nu_{21} \quad (25)$$

The line profile is

$$\phi(\nu) = \frac{1}{\delta\nu} \text{ for } \nu \in \left[\nu_{21} - \frac{\delta\nu}{2}, \nu_{21} + \frac{\delta\nu}{2}\right], \quad (26)$$

and  $\phi(\nu) = 0$  otherwise. For a frequency within the range of 21cm radiation passing through the wake the relative brightness temperature is given by (13). This makes the origin of the  $(\sin \theta)^{-2}$  factor manifest.

Any actual measurement will have a finite frequency resolution. If we integrate over a frequency interval larger than  $\delta\nu$ , the  $(\sin \theta)^{-2}$  factor will cancel as it must. If we have a very small frequency resolution  $R$ , then the brightness temperature density at a fixed  $\nu$  will increase as  $\theta$  decreases until  $\delta\nu$  becomes smaller than  $R$ . From that point onwards, the result will be independent of  $\theta$ . Thus there is never any divergence associated with  $\theta \rightarrow 0$ .

### Acknowledgments

This work is supported in part by a NSERC Discovery Grant, by funds from the CRC Program, and by the FQRNT Programme de recherche pour les enseignants de collège.

- 
- [1] R. H. Brandenberger, R. J. Danos, O. F. Hernández and G. P. Holder, “The 21 cm Signature of Cosmic String Wakes,” JCAP **1012**, 028 (2010) [arXiv:1006.2514 [astro-ph.CO]].
- [2] O. F. Hernández, Y. Wang, R. Brandenberger and J. Fong, “Angular 21 cm Power Spectrum of a Scaling Distribution of Cosmic String Wakes,” JCAP **1108**, 014 (2011) [arXiv:1104.3337 [astro-ph.CO]].
- [3] C. Dvorkin, M. Wyman and W. Hu, “Cosmic String constraints from WMAP and SPT,” arXiv:1109.4947 [astro-ph.CO].
- [4] L. Pogosian, S. H. H. Tye, I. Wasserman and M. Wyman, “Observational constraints on cosmic string production during brane inflation,” Phys. Rev. D **68**, 023506 (2003) [Erratum-ibid. D **73**, 089904 (2006)] [arXiv:hep-th/0304188]; M. Wyman, L. Pogosian and I. Wasserman, “Bounds on cosmic strings from WMAP and SDSS,” Phys. Rev. D **72**, 023513 (2005) [Erratum-ibid. D **73**, 089905 (2006)] [arXiv:astro-ph/0503364]; A. A. Fraisse, “Limits on Defects Formation and Hybrid Inflationary Models with Three-Year WMAP Observations,” JCAP **0703**, 008 (2007) [arXiv:astro-ph/0603589]; U. Seljak, A. Slosar and P. McDonald, “Cosmological parameters from combining the Lyman-alpha forest with CMB, galaxy clustering and SN constraints,” JCAP **0610**, 014 (2006) [arXiv:astro-ph/0604335]; R. A. Battye, B. Garbrecht and A. Moss, “Constraints on supersymmetric models of hybrid inflation,” JCAP **0609**, 007 (2006) [arXiv:astro-ph/0607339]; R. A. Battye, B. Garbrecht, A. Moss and H. Stoica, “Constraints on Brane Inflation and Cosmic Strings,” JCAP **0801**, 020 (2008) [arXiv:0710.1541 [astro-ph]]; N. Bevis, M. Hindmarsh, M. Kunz and J. Urrestilla, “CMB power spectrum contribution from cosmic strings using field-evolution simulations of the Abelian Higgs model,” Phys. Rev. D **75**, 065015 (2007) [arXiv:astro-ph/0605018]; N. Bevis, M. Hindmarsh, M. Kunz and J. Urrestilla, “Fitting CMB data with cosmic strings and inflation,” Phys. Rev. Lett. **100**, 021301 (2008) [astro-ph/0702223 [ASTRO-PH]]; R. Battye and A. Moss, “Updated constraints on the cosmic string tension,” Phys. Rev. D **82**, 023521 (2010) [arXiv:1005.0479 [astro-ph.CO]]; J. Urrestilla, N. Bevis, M. Hindmarsh and M. Kunz, “Cosmic string parameter constraints and model analysis using small scale Cosmic Microwave Background data,” JCAP **1112**, 021 (2011) [arXiv:1108.2730 [astro-ph.CO]].
- [5] J. Canny, “A computational approach to edge detection”, IEEE Trans. Pattern Analysis and Machine Intelligence **8**, 679 (1986).
- [6] S. Amsel, J. Berger and R. H. Brandenberger, “Detecting Cosmic Strings in the CMB with the Canny Algorithm,” JCAP **0804**, 015 (2008) [arXiv:0709.0982 [astro-ph]]; A. Stewart and R. Brandenberger, “Edge Detection, Cosmic Strings and the South Pole Telescope,” JCAP **0902**, 009 (2009) [arXiv:0809.0865 [astro-ph]]; R. J. Danos and R. H. Brandenberger, “Canny Algorithm, Cosmic Strings and the Cosmic Microwave Background,” Int. J. Mod. Phys. D **19**, 183 (2010) [arXiv:0811.2004 [astro-ph]]; R. J. Danos and R. H. Brandenberger, “Searching for Signatures of Cosmic Superstrings in the CMB,” JCAP **1002**, 033 (2010) [arXiv:0910.5722 [astro-ph.CO]].
- [7] S. Sarangi and S. H. H. Tye, “Cosmic string production towards the end of brane inflation,” Phys. Lett. B **536**, 185 (2002) [arXiv:hep-th/0204074].

- [8] R. Jeannerot, “A Supersymmetric SO(10) Model with Inflation and Cosmic Strings,” Phys. Rev. D **53**, 5426 (1996) [arXiv:hep-ph/9509365];  
R. Jeannerot, J. Rocher and M. Sakellariadou, “How generic is cosmic string formation in SUSY GUTs,” Phys. Rev. D **68**, 103514 (2003) [arXiv:hep-ph/0308134].
- [9] R. H. Brandenberger and C. Vafa, “Superstrings In The Early Universe,” Nucl. Phys. B **316**, 391 (1989).;  
A. Nayeri, R. H. Brandenberger and C. Vafa, “Producing a scale-invariant spectrum of perturbations in a Hagedorn phase of string cosmology,” Phys. Rev. Lett. **97**, 021302 (2006) [arXiv:hep-th/0511140].
- [10] R. H. Brandenberger, “String Gas Cosmology,” arXiv:0808.0746 [hep-th].
- [11] A. Vilenkin and E.P.S. Shellard, *Cosmic Strings and other Topological Defects* (Cambridge Univ. Press, Cambridge, 1994).
- [12] M. B. Hindmarsh and T. W. B. Kibble, “Cosmic strings,” Rept. Prog. Phys. **58**, 477 (1995) [arXiv:hep-ph/9411342].
- [13] R. H. Brandenberger, “Topological defects and structure formation,” Int. J. Mod. Phys. A **9**, 2117 (1994) [arXiv:astro-ph/9310041].
- [14] A. Albrecht and N. Turok, “Evolution Of Cosmic Strings,” Phys. Rev. Lett. **54**, 1868 (1985);  
D. P. Bennett and F. R. Bouchet, “Evidence For A Scaling Solution In Cosmic String Evolution,” Phys. Rev. Lett. **60**, 257 (1988);  
B. Allen and E. P. S. Shellard, “Cosmic String Evolution: A Numerical Simulation,” Phys. Rev. Lett. **64**, 119 (1990);  
C. Ringeval, M. Sakellariadou and F. Bouchet, “Cosmological evolution of cosmic string loops,” JCAP **0702**, 023 (2007) [arXiv:astro-ph/0511646];  
V. Vanchurin, K. D. Olum and A. Vilenkin, “Scaling of cosmic string loops,” Phys. Rev. D **74**, 063527 (2006) [arXiv:gr-qc/0511159].
- [15] M. Pagano and R. Brandenberger “The 21cm Signature of a Cosmic String Loop” arXiv:1201.5695 [astro-ph.CO].
- [16] J. Silk and A. Vilenkin, “Cosmic Strings And Galaxy Formation,” Phys. Rev. Lett. **53**, 1700 (1984);  
M. Rees, “Baryon concentrations in string wakes at  $z \geq 200$ : implications for galaxy formation and large-scale structure,” Mon. Not. R. astr. Soc. **222**, 27p (1986);  
T. Vachaspati, “Cosmic Strings and the Large-Scale Structure of the Universe,” Phys. Rev. Lett. **57**, 1655 (1986);  
A. Stebbins, S. Veeraraghavan, R. H. Brandenberger, J. Silk and N. Turok, “Cosmic String Wakes,” Astrophys. J. **322**, 1 (1987);  
J. C. Charlton, “Cosmic String Wakes and Large Scale Structure,” Astrophys. J. **325**, 52 (1988);  
T. Hara and S. Miyoshi, “Formation of the First Systems in the Wakes of Moving Cosmic Strings,” Prog. Theor. Phys. **77**, 1152 (1987);  
T. Hara and S. Miyoshi, “Flareup of the Universe After Z Approximately  $10^{*2}$  for Cosmic String Model,” Prog. Theor. Phys. **78**, 1081 (1987);  
T. Hara and S. Miyoshi, “Large Scale Structures and Streaming Velocities Due to Open Cosmic Strings,” Prog. Theor. Phys. **81**, 1187 (1989).
- [17] Y. B. Zeldovich, “Gravitational instability: An Approximate theory for large density perturbations,” Astron. Astrophys. **5**, 84 (1970).
- [18] R. H. Brandenberger, L. Perivolaropoulos and A. Stebbins, “Cosmic Strings, Hot Dark Matter and the Large-Scale Structure of the Universe,” Int. J. Mod. Phys. A **5**, 1633 (1990);  
L. Perivolaropoulos, R. H. Brandenberger and A. Stebbins, “Dissipationless Clustering Of Neutrinos In Cosmic String Induced Wakes,” Phys. Rev. D **41**, 1764 (1990).
- [19] A. Sornborger, R. H. Brandenberger, B. Fryxell and K. Olson, “The structure of cosmic string wakes,” Astrophys. J. **482**, 22 (1997) [arXiv:astro-ph/9608020].
- [20] B. Zygelman, “Hyper-fine Level-changing Collisions of Hydrogen Atoms and Tomography of the Dark Age Universe”, Astrophys. J. **622**, 1356 (2005);  
S. Furlanetto and M. Furlanetto, “Spin Exchange Rates in Electron-Hydrogen Collisions,” Mon. Not. Roy. Astron. Soc. **374**, 547 (2007) [arXiv:astro-ph/0608067].
- [21] O. F. Hernández and G. P. Holder, “The High-Redshift Neutral Hydrogen Signature of an Anisotropic Matter Power Spectrum,” JCAP **1109**, 031 (2011) [arXiv:1104.5403 [astro-ph.CO]].
- [22] M. F. Morales, “Power spectrum sensitivity and the design of epoch of reionization observatories,” Astrophys. J. **619**, 678 (2005) [arXiv:astro-ph/0406662].
- [23] D. J. Fixsen *et al.*, “ARCADE 2 Measurement of the Extra-Galactic Sky Temperature at 3-90 GHz,” arXiv:0901.0555 [astro-ph.CO].
- [24] E. McDonough and R. H. Brandenberger, “Searching for Signatures of Cosmic String Wakes in 21cm Redshift Surveys using Minkowski Functionals,” arXiv:1109.2627 [astro-ph.CO].